

# Reionization Feedback and the Photoevaporation of Intergalactic Clouds

Paul R. Shapiro,<sup>1,2</sup> Alejandro C. Raga,<sup>2</sup> and Garrelt Mellema<sup>3</sup>

<sup>1</sup>*Department of Astronomy, University of Texas, Austin, TX 78712, USA*

<sup>2</sup>*Instituto de Astronomía-UNAM, Apdo Postal 70-264, 04510 México D. F., México*

<sup>3</sup>*Stockholm Observatory, S-133 36 Saltsjöbaden, Sweden*

**Abstract.** Energy released by a small fraction of the baryons in the universe, which condensed out of while the IGM was cold, dark, and neutral, reheated and reionized it, exposing gas clouds within it to the glare of ionizing radiation. The first gas dynamical simulations of the photoevaporation of an intergalactic cloud by a quasar, including radiative transfer, are presented, along with a few observational diagnostics.

## 1 Reionization, Reheating, and Feedback

The Gunn-Peterson limit implies that the IGM was reionized and reheated by  $z \sim 5$ , by energy released by objects which previously condensed out of the background and formed stars, AGNs or some other sources. This exerted a negative feedback on the rate of collapse of gas out of the background IGM by raising the Jeans mass there and affected the appearance and evolution of the IGM and the structure which subsequently collapsed out of it. How early could starlight have reionized the IGM? Shapiro and Giroux attempted to answer this question by solving linear equations for the growth of density fluctuations in the IGM and using a Press-Schechter approach to determine the baryon fraction which had collapsed out at any epoch, releasing energy to reheat and reionize the IGM, coupled to a detailed numerical evolution of the thermal and ionization balance of a coarse-grained, spatially-averaged IGM and the equation of radiative transfer for the ionizing radiation background, including the opacity of the observed quasar absorption line gas, as described in [1], [2], and [3]. The maximum-possible efficiency was assumed for energy release by massive stars, which form at a rate proportional to the rate of collapse of baryons out of the IGM and stop forming when they have enriched the collapsed fraction with a solar abundance of heavy elements, in a flat, COBE-normalized, standard CDM model ( $\Omega_B = 0.06$ ,  $h = 0.5$ ,  $\Omega = 1$ ). The IGM was found to reheat by  $z_h \sim 65$  to  $T_{\text{IGM}} \sim 10^{3.5}\text{K}$  when the collapsed baryon fraction was only  $f_{\text{coll}} \approx 10^{-4}$ , while the H atom ionization breakthrough was  $z_b \sim 50$  when  $f_{\text{coll}} \sim 10^{-3}$ , implying a net metallicity averaged over all baryons in the universe at these epochs equal to these values of  $f_{\text{coll}}$ , in solar units

[3]. Since the COBE-normalization is almost twice that typically assumed in recent simulations of the Lyman alpha forest and galaxy formation, our results are *conservative* in the sense of maximizing  $z_b$ ; a lower initial amplitude would make reionization and reheating occur a little later than this. In my talk, I also presented ASPH simulations by Shapiro and Martel which demonstrated that global reheating can significantly affect the small-scale structure formation responsible for quasar absorption line gas ([3],[4],[5]). This contribution is too brief to present that material, but I refer the reader to [3] for a summary. Here we will focus, instead, on new work on the effects of photoionization.

## 2 The Photoevaporation of Intergalactic Clouds

The first sources of ionizing radiation which turned on in the neutral (i.e. postrecombination) IGM prior to  $z \sim 5$  resulted in isolated, expanding H II regions. The expansion and eventual overlap of the weak, R-type cosmological ionization fronts bounding these H II regions was previously described analytically by treating the IGM as a uniform, cosmologically expanding gas ([6],[7]). The density fluctuations required to explain galaxy formation and the Lyman alpha forest were accounted for approximately by treating the IGM as “clumpy,” with a universal clumping factor. That approximation is correct in the limit in which the clumps are either too small to “self-shield” or else constitute only a small fraction of the total mass inside the HII region. It does not, however, address the possible dynamical consequences for the clumps, themselves, of the passage of I-fronts. In what follows, we present the first simulations of the gas dynamics and radiative transfer of an intergalactic cloud overtaken by a cosmological I-front.

The fate of this cloud depends fundamentally on whether or not it can shield itself against the incident radiation from the external source responsible for the intergalactic I-front. If the cloud size exceeds the “Strömgren length” (the length of a column of gas within which the unshielded arrival rate of ionizing photons just balances the total recombination rate), it can trap the I-front. In that case, the weak R-type I-front which swept into the cloud initially, moving supersonically with respect to gas both ahead and behind, decelerates to the sound speed of the ionized gas before it can exit the cloud, thereby becoming a weak, D-type front preceded by a shock. Typically, the side of the cloud which faces the radiation source expels a supersonic wind which causes the remaining cloud material to be accelerated away from the source by the so-called “rocket effect” as the cloud photoevaporates (cf.[8]). For a uniform gas of H density  $n_{H,c}$ , located a distance  $r_{\text{Mpc}}$  (in Mpc) from a UV source emitting  $N_{\text{ph},56}$  ionizing photons per second (in units of  $10^{56}\text{s}^{-1}$ ), the Strömgren length is only  $\ell_S \cong (50 \text{ pc})(N_{\text{ph},56}/r_{\text{Mpc}}^2)(n_{H,c}/0.1 \text{ cm}^{-3})^{-2}$ . Gas bound to dark matter halos whose virial temperature is less than  $10 \text{ km s}^{-1}$  will photoevaporate unimpeded by gravity. For larger halos gravity competes with the effects of photoevaporation.

As a first study of these important effects, we have simulated the photo-evaporation of a uniform, spherical, neutral, intergalactic cloud of gas mass  $1.5 \times 10^6 M_{\odot}$ , radius  $R_c = 0.5$  kpc, density  $n_{\text{H,c}} = 0.1 \text{ cm}^{-3}$  and  $T = 100$  K, in which self-gravity is unimportant, located 1 Mpc from a quasar with emission spectrum  $F_{\nu} \propto \nu^{-1.8}$  ( $\nu > \nu_{\text{H}}$ ) and  $N_{\text{ph}} = 10^{56} \text{ s}^{-1}$ , initially in pressure balance with an ambient IGM of density  $0.001 \text{ cm}^{-3}$  which at time  $t = 0$  has just been photoionized by the passage of the intergalactic R-type I-front generated when the quasar turned on. Apart from H and He, the cloud also contains heavy elements at  $10^{-3}$  times the solar abundance. Our simulations in 2D, axisymmetry use an Eulerian hydro code (called CORAL), with Adaptive Mesh Refinement and a Riemann solver based on the Van Leer flux-splitting algorithm, which solves nonequilibrium ionization rate equations (for H, He, C, N, O, Ne, and S) and includes an explicit treatment of radiative transfer which takes account of bound-free opacity of H and He ([9],[10],[11]). Our grid size in  $(r, z)$  was  $128 \times 512$  cells (fully refined). Figure 1 shows the structure of the cloud 50 Myr after it was overtaken by the quasar's I-front as it sweeps past the cloud in the IGM. Since  $\ell_S \ll R_c$  initially, the cloud traps the I-front, as described above, and drives a supersonic wind from the surface facing the quasar. It takes more than 100 Myr to evaporate the cloud, accelerating it to  $10^3$  of  $\text{km s}^{-1}$  in the process. Figure 2 shows selected observable diagnostics, including column densities of H I, He I and II seen along the symmetry axis at different times and the spatial variation of the relative abundances of selected metal ions at 50 Myr. The cloud starts as a high-column-density Lyman Limit absorber, but ends with the H I column density of a Lyman alpha forest cloud, with  $[\text{He II}]/[\text{H I}] \sim 10^2$  and metal ions.

**Acknowledgements.** This work was supported by NASA Grant NAG5-2785 and NSF Grant ASC-9504046, and was made possible by a UT Dean's Fellowship and a National Chair of Excellence, UNAM, Mexico in 1997 for PRS. PRS is also grateful to Hugo Martel and Mark Giroux for their collaboration in the work referred to in §1, which space did not permit us to include here.

## References

- [1] Shapiro, P. R., Giroux, M. L., & Babul, A. 1994, ApJ, 427, 25.
- [2] Giroux, M. L., & Shapiro, P. R. 1996, ApJ Suppl., 102, 191.
- [3] Shapiro, P. R. 1995, in *The Physics of the Interstellar Medium*, eds. A. Ferrara, C. F. McKee, C. Heiles, and P. R. Shapiro (ASP Conf. Vol. 80), 55–97.
- [4] Shapiro, P. R., & Martel, H. 1995, in *Dark Matter*, eds. S. S. Holt and C. L. Bennett (AIP Conf. Proc. 336), pp. 446–449.
- [5] Shapiro, P. R., & Martel, H. 1997, in preparation.
- [6] Shapiro, P. R. 1986, PASP, 98, 1014.
- [7] Shapiro, P. R., & Giroux, M. L. 1987, ApJ, 321, L107.
- [8] Spitzer, L. 1978, *Physical Processes in the Interstellar Medium* (Wiley).
- [9] Mellema, G., Raga, A. C., Canto, J., Lundqvist, P., Balick, B., Steffen, W., & Noriega-Crespo, A. 1997, A&A, submitted.
- [10] Raga, A. C., Mellema, G., & Lundquist, P. 1977, ApJ Suppl., 109, 517.
- [11] Raga, A. C., Taylor, S. D., Cabrit, S., & Biro, S. 1995, A&A, 296, 833.

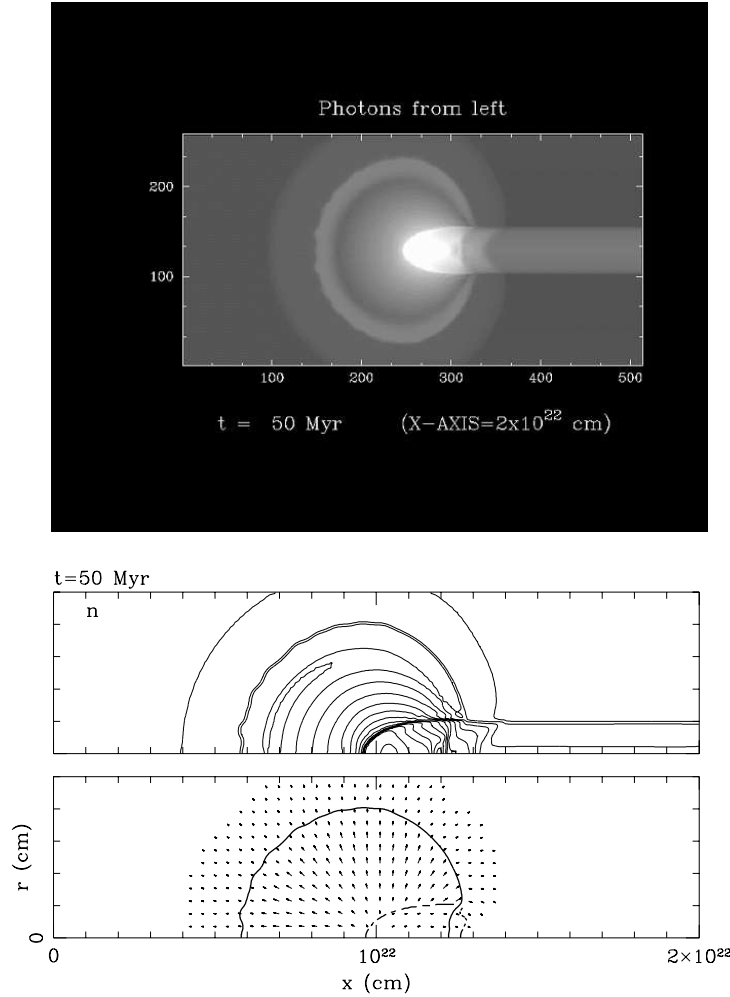


Figure 1: THE PHOTOEVAPORATION OF AN INTERGALACTIC GAS CLOUD BY IONIZING RADIATION FROM A NEARBY QUASAR. (a) Results 50 Myr after the quasar, located 1 Myr away along the x-axis to the left of the computational box, first turns on. (a) (upper box) Shaded isodensity contours with logarithmic spacing, of the total atomic (HI) density  $n$  (highest = white, lowest = black). (b) (lower panels) contour plots of atomic density (upper), logarithmically spaced, and (lower) velocity arrows are plotted for velocities larger than 5 km/s, with length proportional to velocity. The solid line shows current extent of the original cloud matter and dashed line is the I-front (50% H ionization contour).

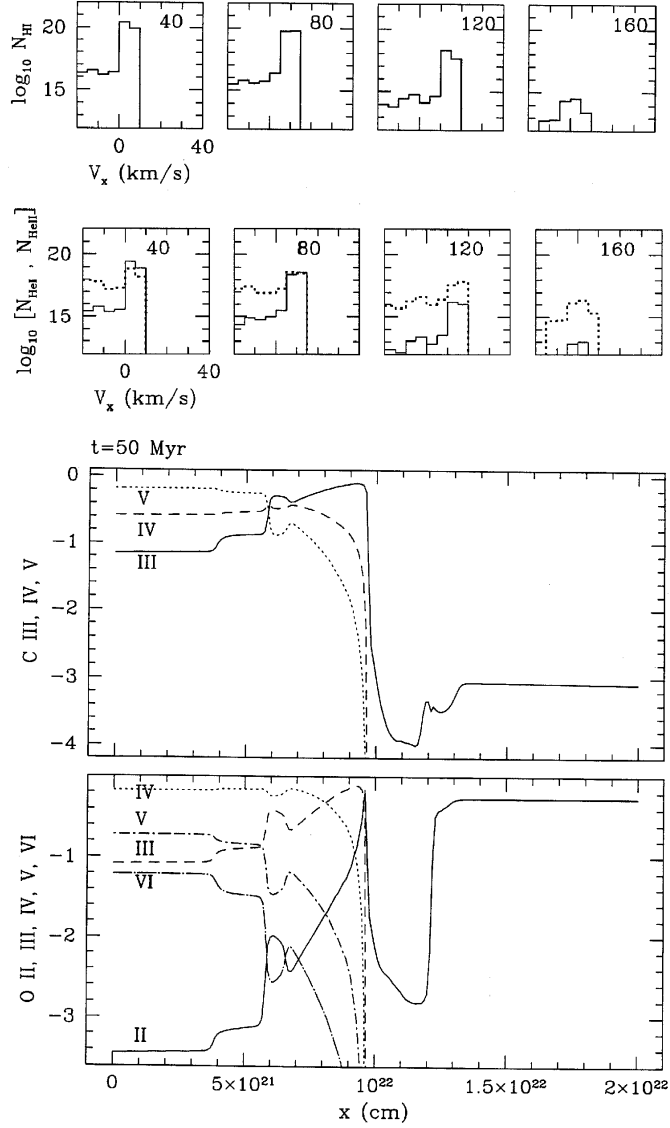


Figure 2: PHOTOEVAPORATING CLOUD: OBSERVATIONAL DIAGNOSTICS. (a) Column Densities of H I (top panels) and of He I (solid) and II (dotted) (middle panels) versus velocity as measured along the  $x$ -axis at  $r = 0$ . Each box labelled with time (in Myrs) since the QSO turned on. (b) (bottom panels) Carbon and Oxygen ionic fractions along this symmetry axis at  $t = 50$  Myr.